THE JOURNAL OF BIOLOGICAL CHEMISTRY VOL. 287, NO. 7, pp. 4602–4608, February 10, 2012

Nucleophilic Participation of Reduced Flavin Coenzyme in Mechanism of UDP-galactopyranose Mutase*[S]

Received for publication, October 11, 2011, and in revised form, December 1, 2011 Published, JBC Papers in Press, December 20, 2011, DOI 10.1074/jbc.M111.312538

He G. Sun, Mark W. Ruszczycky, Wei-chen Chang, Christopher J. Thibodeaux, and Hung-wen Liu[1]

From the Division of Medicinal Chemistry, College of Pharmacy, Department of Chemistry and Biochemistry and Institute of Cellular and Molecular Biology, University of Texas, Austin, Texas 78712-0128

Background: UDP-galactopyranose mutase (UGM) requires the reduced FAD coenzyme to interconvert UDP-galactopyranose and UDP-galactofuranose.
Results: Structural perturbations of the coenzyme inhibit bond cleavage in the substrate.
Conclusion: Concerted bond breaking and formation between substrate and coenzyme occur during UGM catalysis.
Significance: Mechanistic understanding of UGM offers new insight for clinically relevant inhibitor design.

UDP-galactopyranose mutase (UGM) requires reduced FAD (FAD_{red}) to catalyze the reversible interconversion of UDP-galactopyranose (UDP-Gal*p*) and UDP-galactofuranose (UDP-Gal*f*). Recent structural and mechanistic studies of UGM have provided evidence for the existence of an FAD-Gal*f*/*p* adduct as an intermediate in the catalytic cycle. These findings are consistent with Lewis acid/base chemistry involving nucleophilic attack by N5 of FAD_{red} at C1 of UDP-Gal*f*/*p*. In this study, we employed a variety of FAD analogues to characterize the role of FAD_{red} in the UGM catalytic cycle using positional isotope exchange (PIX) and linear free energy relationship studies. PIX studies indicated that UGM reconstituted with 5-deaza-FAD_{red} is unable to catalyze PIX of the bridging C1–OP_β oxygen of UDP-Gal*p*, suggesting a direct role for the FAD_{red} N5 atom in this process. In addition, analysis of kinetic linear free energy relationships of k_{cat} *versus* the nucleophilicity of N5 of FAD_{red} gave a slope of $\rho = -2.4 \pm 0.4$. Together, these findings are most consistent with a chemical mechanism for UGM involving an S_N2-type displacement of UDP from UDP-Gal*f*/*p* by N5 of FAD_{red}.

UDP-galactopyranose mutase (UGM)[2] is a flavoprotein that catalyzes the isomerization of UDP-galactopyranose (UDP-Gal*p*; **1** in Fig. 1) and UDP-galactofuranose (UDP-Gal*f*; **2**). This reaction is essential for many pathogenic species of bacteria, protozoa, and fungi because UDP-Gal*f* serves as the activated Gal*f* donor during cell wall biosynthesis in these organisms (1, 2). Of particular clinical importance is the causative agent of tuberculosis, *Mycobacterium tuberculosis*, the cell wall of which possesses a galactan chain of ~35 Gal*f* residues that is essential for viability (3). Given the global prevalence of tuberculosis (World Health Organization Media Center) (4) and the increasing incidence of multidrug-resistant strains (6), UGM has become an attractive drug target because mammalian glycans do not contain Gal*f* residues. UGM has also attracted much attention because it requires a reduced FAD coenzyme (FAD_{red}; **3**) to catalyze a reversible ring contraction/expansion reaction that is redox-neutral (7). This has raised questions about the catalytic function of the coenzyme during turnover.

Several previous studies have provided important insights into the chemical mechanism of the UGM-catalyzed reaction. Using positional isotope exchange (PIX) studies, Blanchard and co-workers (8) demonstrated that the anomeric C1–OP_β bond is broken and reformed during turnover. Using $NaCNBH_3$ as a chemical quenching agent to trap species **9** (Fig. 1), Kiessling and co-workers (9, 10) provided evidence for the intermediacy of the iminium ion (**7**) in the UGM catalytic cycle. Species **7** is likely derived from the FAD-substrate adducts **6** and **8**, where N5 of the flavin is covalently linked to the anomeric carbon of the substrate (9, 10). Structures of reduced UGM determined in the presence of UDP-Gal*p* by saturation transfer difference NMR spectroscopy (11) and x-ray crystallography (10) revealed that N5 of FAD_{red} is in close proximity to the anomeric carbon of the substrate, providing compelling evidence for the participation of N5 in nucleophilic attack at C1 of the substrate to form **6** and **8** during turnover.

Three mechanistic hypotheses have been proposed to explain the formation of **6** and **8** (Fig. 1). Generation of these intermediates may occur via nucleophilic attack by N5 of FAD_{red} at the anomeric carbon of **1** (or **2**) concerted with cleavage of the C1–OP_β bond (Fig. 1, *path A*), which is reminiscent of typical S_N2-type substitutions. Alternatively, formation of **6** and **8** may take place in a stepwise fashion similar to S_N1-type substitutions (Fig. 1, *path B*), where elimination of UDP to produce an oxocarbenium intermediate (such as **4**) precedes the nucleophilic attack by N5. It is also possible that the electron-deficient nature of **4** could facilitate single-electron transfer (SET) from FAD_{red} to form a radical pair (such as **5** and **10**), followed by covalent bond formation to afford **6** and **8** (Fig. 1, *path C*). Indirect evidence for an oxocarbenium intermediate

* This work was supported, in whole or in part, by National Institutes of Health Grants GM035906 and GM054346 and Fellowship Award F32AI082906 from NIAID (to M. W. R.). This work was also supported by Welch Foundation Grant F-1511.
[S] This article contains supplemental data, Figs. S1–S3, Tables S1–S6, and additional equations and references.
[1] To whom correspondence should be addressed: University of Texas, 2409 University Ave., PHR 3.206B, Austin, TX 78712-0128. Fax: 512-471-2746; E-mail: h.w.liu@mail.utexas.edu.
[2] The abbreviations used are: UGM, UDP-galactopyranose mutase; UDP-Gal*p*, UDP-galactopyranose; UDP-Gal*f*, UDP-galactofuranose; FAD_{red}, reduced FAD; PIX, positional isotope exchange; SET, single-electron transfer; LFER, linear free energy relationship.

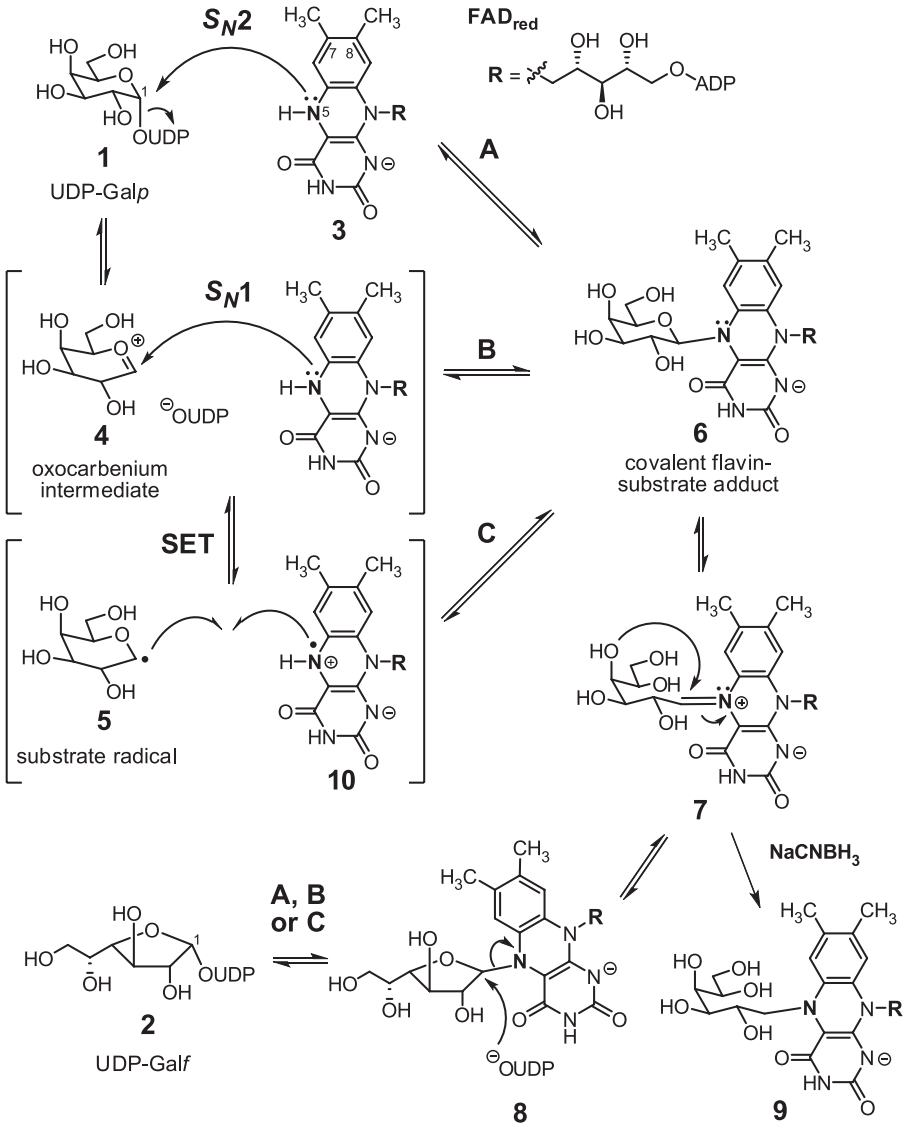

FIGURE 1. **Putative chemical mechanisms for UGM catalysis.**

has come in the form of a significant rate reduction observed with UDP-[2-F]Gal*f* (12) and the inability of UGM to displace UDP from the linear substrate analog UDP-galactitol (13).

In this study, we employed PIX and linear free energy relationships (LFERs) to further investigate the role of N5 of FAD_{red} during UGM catalysis. To determine whether N5 is indeed necessary for cleavage of the anomeric bond of UDP-Gal*p*, PIX was monitored for the double-labeled UDP-Gal*p* substrate in the presence of UGM reconstituted with reduced 5-deaza-FAD. The results were then corroborated by considering the perturbations to the rate of isomerization imposed upon changing the nucleophilicity of N5. Together, the results of these experiments are most consistent with an S_N2-type displacement of UDP from the substrate by N5 of FAD_{red} (Fig. 1, *path A*).

EXPERIMENTAL PROCEDURES

UGM Expression and Purification—The *glf* gene encoding UGM was introduced into a pET-24b$^+$ vector to generate the recombinant pQZ-1 plasmid (7). The plasmid was then transformed into *Escherichia coli* BL21 Star^{TM} (DE3) for overexpression of UGM as a C-terminal His_6 fusion protein. Cells were cultured in LB medium with 50 mg/liter kanamycin at 37 °C until the absorbance at 600 nm reached 0.6. Protein overexpression was induced by the addition of isopropyl β-D-thiogalactopyranoside to 0.1 mM, and the culture was allowed to incubate for an additional 18 h at 18 °C. The cells were then harvested by centrifugation, disrupted by sonication, and purified using nickel-nitrilotriacetic acid resin (Qiagen). UGM was purified as the holoenzyme with a bright yellow color and a distinct UV-visible absorption profile characteristic of tightly bound FAD. The purified enzyme was then flash-frozen in storage buffer (100 mM potassium P_i (pH 7.5) containing 15% glycerol) and stored at −80 °C.

*Preparation of Double-labeled UDP-Gal*p—Double-labeled UDP-Gal*p* was prepared according to published methods (8), where the double labels were introduced by incubating 100 mg of D-[1-^{13}C]galactose (99%; Cambridge Isotope Laboratories) in 200 μl of $H_2{}^{18}O$ (95%, normalized; Fluka) at 55 °C for 2 days. This led to ~80% incorporation of ^{18}O at C1 as determined by mass spectrometry. A solution of 80 mM double-labeled galac-

tose was then treated with pyruvate kinase and galactose kinase in the presence of 125 mM phosphoenolpyruvate and 6 mM ATP in 50 mM Tris buffer (pH 7.5) to generate [1-^{13}C,1-^{18}O]galactose 1-phosphate. The enzymes were removed by filtration (YM-10 membrane) following complete consumption of the labeled galactose as monitored by TLC. The filtrate was adjusted to pH 8.5 and treated with galactose-1-phosphate uridyltransferase, UDP-glucose pyrophosphorylase, and inorganic pyrophosphatase in the presence of 0.6 mM UDP-glucose and 100 mM UTP to form UDP-[1-^{13}C,1-^{18}O]Gal*p*. The reaction was monitored by HPLC (see below for conditions). Enzymes were then removed by filtration (YM-10 membrane), and the product was purified using a DEAE-cellulose column eluted with a 0–0.1 M gradient of NH_4HCO_3 in water. The isolated UDP-Gal*p* was determined to be 95% pure based on HPLC analysis. The extent of isotopic double-label incorporation into the UDP-Gal*p* product was determined by ^{1}H NMR and ^{13}C NMR spectrometries and confirmed by high resolution electrospray ionization mass spectrometry (negative-ion mode), demonstrating peaks at *m*/*z* 566.0518 and 568.0530, corresponding to the ^{16}O (calculated *m*/*z* 566.0511) and ^{18}O (calculated *m*/*z* 568.0553) isotopologues, respectively.

Preparation of 7/8-Substituted FAD Analogues—The 7/8-substituted FAD analogues used in this study were prepared according to published methods (14). The identity of each compound was verified by ^{1}H NMR and ^{31}P NMR spectroscopies as well as by high resolution electrospray ionization mass spectrometry.

Preparation of Apo-UGM and Reconstitution with Other FAD Analogues—FAD was removed from the purified enzyme by the addition of a 2.6-fold volume excess of 3 M KBr in 20% glycerol to a 10 mg/ml enzyme stock in storage buffer (15). The resulting mixture was incubated on ice for 2 min before precipitating the enzyme by the addition of a 1.8-fold volume excess of saturated ammonium sulfate (pH 2.5). The enzyme precipitate was pelleted by centrifugation at 18,000 × *g* for 10 min. The clear yellow supernatant containing released FAD was decanted, and the protein pellet was redissolved in 4 ml of storage buffer. The high salt treatment was repeated a second time, and the resulting apo-UGM was dialyzed against storage buffer. Reconstitution of UGM with FAD analogues was carried out by incubating a 2.5 mg/ml solution of apo-UGM with an excess of flavin cofactor for 15 min at room temperature. The reconstituted enzyme/cofactor solution was then diluted with storage buffer to a concentration compatible with the enzyme assays. In the LFER studies, the molar ratio of cofactor to apo-UGM was ~100:1. Enzyme concentrations were determined by the Bradford assay using bovine serum albumin as the protein standard.

PIX Time Course Experiments—PIX experiments were carried out at 27 °C in NMR tubes containing 50 mM potassium P_i (pH 7.5), 10% D_2O (for locking the ^{13}C NMR signal), 7 mM $Na_2S_2O_4$, and ~14 mM double-labeled UDP-Gal*p* in a total volume of ~630 μl. Apo-UGM was preincubated with the respective cofactor for 15 min before dilution into the reaction solution. In the 5-deaza-FAD/UGM and apo-UGM samples, the final enzyme concentration was 15 μM, and the 5-deaza-FAD concentration was ~820 μM. In the FAD/UGM positive control, the final enzyme and FAD concentrations were 10 and 220 μM, respectively. All ^{13}C NMR spectra were recorded using a 600-MHz Varian NMR spectrometer except for the reaction with apo-UGM, which was recorded using a 500-MHz Varian NMR spectrometer, at the Nuclear Magnetic Resonance Facility of the Department of Chemistry and Biochemistry of the University of Texas at Austin.

UGM Kinetic Assay—Initial rates for the conversion of UDP-Gal*f* to UDP-Gal*p* by reconstituted UGM were determined according to a previously described discontinuous assay (12). Reactions were run in 50 mM potassium P_i (pH 7.5) containing 7 mM $Na_2S_2O_4$ and 10–500 μM UDP-Gal*f* in a total volume of 30 μl. The temperature was maintained at 37 °C using a water bath. Enzyme concentrations varied from 0.015 to 0.2 μM depending on the analogue tested. Reactions were initiated upon the addition of UDP-Gal*f*, quenched with a 3-fold excess of methanol, and centrifuged to remove precipitated protein. The resulting supernatant was dried in a speed vacuum concentrator prior to HPLC analysis. The fraction of reaction was determined based on the relative integrations of the UDP-Gal*f* and UDP-Gal*p* peaks and used to calculate the initial rate of reaction.

HPLC Analysis—HPLC analysis was performed at room temperature using a Varian Microsorb-MV 100-5 C18 column (250 × 4.6 mm) with UV detection at 262 nm. Solvent A contained 50 mM potassium P_i and 2.5 mM tetrabutylammonium hydrogen sulfate (pH 6.9) in H_2O, and solvent B contained 50 mM potassium P_i and 2.5 mM tetrabutylammonium hydrogen sulfate (pH 6.9) in 50% H_2O/acetonitrile. Isocratic elution was performed at 96% solvent A at a flow rate of 1 ml/min.

RESULTS

PIX Equilibration by Apoenzyme Is Not Accelerated in the Presence of 5-Deazaflavin—As described previously (8), the C1 ^{13}C NMR signal of UDP-Gal*p* is split into a doublet by the adjacent β-phosphate and demonstrates an upfield shift of ~0.03 ppm when the anomeric oxygen is replaced with ^{18}O. The resulting two doublets were deconvoluted and integrated using Varian VnmrJ software and a multicomponent fit with Lorentzian line shapes. A ^{13}C NMR example spectrum is provided in supplemental Fig. S2 along with the deconvolution. ^{13}C NMR and mass spectrometry results indicated that the double-labeled UDP-Gal*p* (**11**) was prepared with >99% incorporation of ^{13}C at C1 and 77 ± 4% incorporation of ^{18}O at the bridging C1–OP_β position. All remaining atoms in the substrate were at natural isotopic abundance.

PIX experiments were conducted under reducing conditions (7 mM sodium dithionite) in NMR tubes. The change in the fraction (*f*) of ^{18}O *versus* ^{16}O bound to ^{13}C1 was monitored *versus* time (*t*) by ^{13}C NMR spectroscopy. (^{13}C NMR stack plots are shown in supplemental Fig. S2.) Complete scrambling of the P_β oxygens (Fig. 2) predicts the fraction of ^{18}O at the bridging C1–OP_β position to ultimately reach an equilibrium value of f_{eq} = 0.26 (the product of the initial ^{18}O enrichment in our double-labeled UDP-Gal*p* substrate and the statistical factor of one-third). In the presence of 10 μM UGM reconstituted with FAD_{red}, PIX scrambling (**11** ⇆ **12**) was >90% complete within 20 min of incubation. In contrast, PIX was considerably slower in the presence of either 15 μM apo-UGM or UGM reconsti-

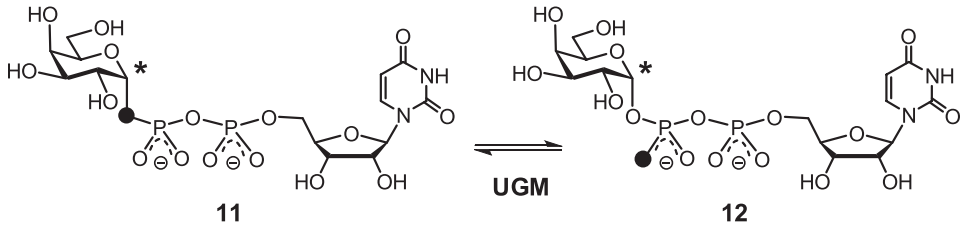

FIGURE 2. **Rationale for PIX experiments.**

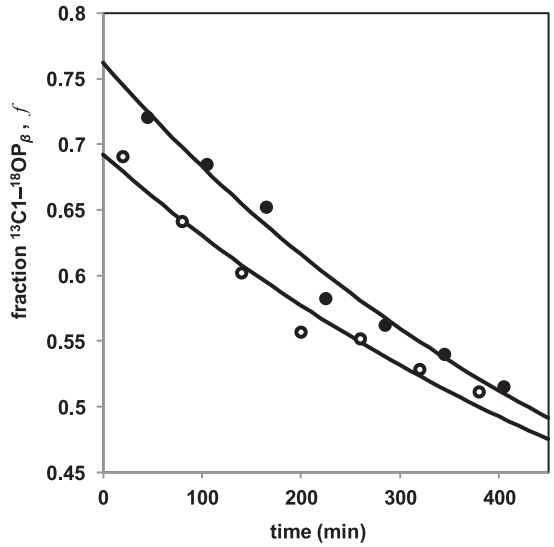

FIGURE 3. **Comparison of PIX rates for apo-UGM (○) *versus* UGM reconstituted with 5-deaza-FAD (●).** Each time course is a plot of the fraction (*f*) of UDP-Gal*p* possessing ^{18}O at the bridging C1–OP_β position as determined by ^{13}C NMR *versus* time. As a reference, the PIX rate was ~100 times faster when UGM was reconstituted with FAD_{red}. Time courses were determined in separate experiments leading to the difference in the ordinate intercepts (see supplemental data for details). Reactions were run at 27 °C in potassium P_i (pH 7.5), 10% D_2O, and 7 mM $Na_2S_2O_4$ with 15 μM enzyme. Progress curves were obtained by fitting Equation 1 to the observed time courses using nonlinear regression.

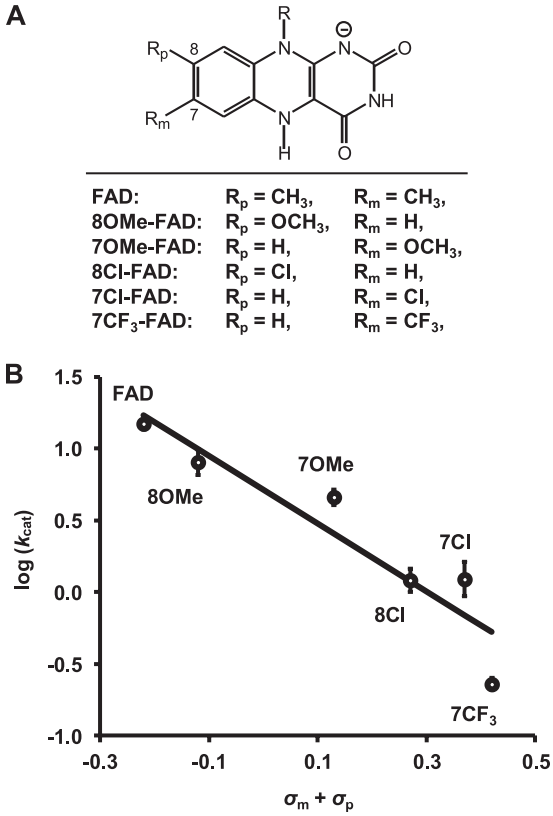

FIGURE 4. **LFER between k_{cat} for UGM-catalyzed isomerization of UDP-Gal*f* to UDP-Gal*p* and electron-withdrawing effects due to *para*/*meta* substitution *versus* N5 of FAD_{red}.** *A*, list of FAD analogues prepared for measuring the LFER. *B*, Hammett plot for the correlation of $\log_{10}(k_{cat})$ *versus* the sum of σ_p and σ_m. The fit was obtained from unweighted least-squares linear regression, and *error bars* denote 1 S.E. of $\log_{10}(k_{cat})$ above and below the observed value. *OMe*, methoxy; *Cl*, chloro; *CF_3*, trifluoromethyl.

tuted with 5-deaza-FAD_{red} (Fig. 3), occurring over a time scale of >7 h. This permitted *f* to be measured every 60 min and subsequently fit using Equation 1 to extract the first-order rate constant for PIX (16),

$$f = f_{eq} + \Delta f \exp(-k_{PIX}t) \quad \text{(Eq. 1)}$$

where f_{eq} is the final value of *f* after complete equilibration of the exchangeable oxygens, and Δf is the difference between the initial value of *f* and f_{eq}. The first-order rate constant (k_{PIX}) describes the approach to the PIX equilibrium under the experimental conditions and is equivalent to the positional exchange rate (17) normalized for the total initial substrate concentration, which was held constant and saturating in the experiments. The parameters k_{PIX} and Δf were both allowed to float during nonlinear fitting, whereas f_{eq} was fixed at 0.26.

The observed values of k_{PIX} for apo-UGM and UGM reconstituted with 5-deaza-FAD_{red} were 0.0015 ± 0.0001 and 0.0017 ± 0.0001 min^{-1}, respectively, ~100-fold smaller than the k_{PIX} for UGM reconstituted with FAD_{red}. These values of k_{PIX} are significantly different from zero ($p < 0.0001$); however, they are not significantly different from one another ($p > 0.3$). No PIX scrambling was observed over a 24-h period when UGM was omitted from the reaction solution. Additional details regarding data fitting and statistical analysis are provided in the supplemental data.

FAD Analogues Yield Negative ρ Value in LFER Studies—Following reconstitution of apo-UGM with each FAD analog (Fig. 4*A*), the turnover number (k_{cat}) for conversion of UDP-Gal*f* to UDP-Gal*p* (Fig. 1, **2** → **1**) was determined from plots of the initial rate (v_i) (12, 15) *versus* substrate concentration (s_i) according to the structural relation (Equation 2),

$$v_i = k_{cat}s_ie_0/(K_m + s_i) \quad \text{(Eq. 2)}$$

where e_0 is the total enzyme concentration, and K_m is the Michaelis constant. Controls were also performed with ratios of 1000:1 for the 8-methoxy-FAD and 7-chloro-FAD analogues *versus* apo-UGM. No significant differences were observed in the fitted kinetic parameters, implying that the

variations in k_{cat} were not a result of subsaturating flavin concentrations. The resulting plot of $\log_{10}(k_{cat})$ *versus* the sum of the substituent constants at positions 7 and 8 of the FAD analogues, denoted σ_m and σ_p, respectively, is shown in Fig. 4*B*. The values of σ_m and σ_p are based on the ionization of phenylacetic acid in water (18); however, substituent constants based on the ionization of benzoic acid in water gave similar results. On the basis of an analysis of variance, we found no evidence for either unequal expression of *para versus meta* effects in the LFER, *i.e.* $\rho_m \neq \rho_p$(19), or non-additivity, *i.e.* higher order terms of σ. The value of the susceptibility factor (ρ) estimated from the linear correlation was -2.4 ± 0.4 and is significantly different from zero ($p < 0.01$). Additional details regarding data fitting and statistical analysis are provided in the supplemental data.

DISCUSSION

Evidence for the cleavage of the anomeric UDP-Gal*p* bond during turnover by UGM was first provided by Blanchard and co-workers (8) using PIX. In this study, incubation of UGM with UDP-[1-^{13}C]Gal*p* enriched with ^{18}O at the bridging oxygen between C1 and the β-phosphate (**11**) was monitored by ^{13}C NMR spectroscopy. When ^{18}O is replaced with ^{16}O at the bridging position in the double-labeled substrate during turnover (see **12**), a well resolved downfield shift of the ^{13}C1 resonance occurs, with the change in the ratio of the ^{13}C–^{18}O and ^{13}C–^{16}O signals indicative of bond cleavage and reformation during catalysis (Fig. 2). It has also been shown that UGM reconstituted with 5-deaza-FAD does not catalyze interconversion of UDP-Gal*f* and UDP-Gal*p* (15). This observation was initially interpreted as support for a mechanism involving SET (Fig. 1, *path C*) because 5-deaza-FAD is restricted to 2-electron processes (20). Nevertheless, this indirect evidence does not exclude the possibility of a nucleophilic role for N5 of FAD_{red} and, in particular, an S_N2-type process if it is required for expulsion of the UDP moiety.

As an initial test of the hypothesis that N5 is directly involved in the cleavage of the anomeric bond of UDP-Gal*p* to form the flavin-substrate adduct (**6** and **8**), we considered the ability of UGM to utilize 5-deaza-FAD to catalyze PIX of the P_β oxygens in UDP-Gal*p*. Reconstitution of apo-UGM with 5-deaza-FAD showed no effect on an observable low background rate of PIX despite the comparable binding affinities of 5-deaza-FAD and FAD_{red} (15). Therefore, the observation that 5-deaza-FAD is unable to substitute for FAD_{red} in catalyzing PIX of the P_β oxygens implies that N5 of FAD_{red} is necessary for cleavage of the anomeric C1–OP_β bond. The background PIX is most likely due to residual (<1%) holo-UGM in the apo-UGM preparation, which is consistent with the tight binding of FAD_{red} to UGM ($K_D < 10$ nM) (15) and the observed formation of UDP-Gal*f* in all reactions (see supplemental data). It should also be noted that PIX would be independent of SET if the reaction were to proceed via the oxocarbenium ion intermediate **4** (Fig. 1, *paths B* and *C*). Thus, the inability of reduced 5-deaza-FAD to promote anomeric bond cleavage/reformation of **1** and **2** cannot be ascribed to an inability to facilitate SET and is more likely due to the absence of N5 serving as the nucleophile in C1–OP_β bond cleavage during the concerted attack at C1 of the substrate (Fig. 1, *path A*).

To characterize the role of N5 of FAD_{red} during the UGM-catalyzed isomerization more closely, we next examined the kinetic LFERs associated with changes in the nucleophilicity of N5. If adduct **6** (or **8**) is formed via an S_N2-type substitution (Fig. 1, *path A*), and if this step is at least partially rate-limiting to steady-state turnover, then changes in the nucleophilicity of N5 should be reflected in the rate of steady-state turnover. In contrast, the rate of steady-state turnover is expected to be much less sensitive to the nucleophilicity of N5 if adduct formation proceeds by an S_N1 or a SET pathway (Fig. 1, *paths B* and *C*), where formation of the oxocarbenium species (**4**) would be substantially rate-limiting. Thus, as the electron density at N5 of FAD_{red} is decreased by substitution of the isoalloxazine moiety, a decrease in the steady-state reaction rate is expected for mechanism A, whereas little or no effect is expected for mechanisms B and C.

To test this hypothesis, several FAD analogues (Fig. 4*A*) containing electron-withdrawing or electron-donating groups at positions 7 and/or 8 of the isoalloxazine moiety (*meta* and *para*, respectively, to the N5 position) were chemoenzymatically synthesized according to published procedures (14). The nucleophilicity of N5 is represented as the sum of the σ_m and σ_p substituent constants for the substituent at the *meta* and *para* positions, respectively, of the FAD analogues. These substituent constants are based on the ionization of phenylacetic acid in water (18). Except for the *para*-methoxy substituent, these values are nearly identical to the Hammett substituent constants obtained for ionization of benzoic acid in water (21). In the case of *p*-methoxy, σ_p is significantly more negative with benzoic acid likely due to hydrogen bond stabilization of a *trans*-quinoidal resonance structure in H_2O (22). Although a better correlation was obtained with the values of σ_m and σ_p based on ionization of phenylacetic acid, the same conclusions were drawn with those based on benzoic acid (see supplemental data). Previous studies of many flavoenzymes (14, 19, 23, 24) and model systems (25) reconstituted with 7- and 8-substituted flavin analogues have established a precedence for significant LFERs correlating Hammett substituent constants with a variety of parameters related to flavin structure and reactivity.

A linear correlation of $\log_{10}(k_{cat})$ for the UGM-catalyzed reaction *versus* the sum of σ_m and σ_p for the FAD analogues was observed with a slope of -2.4 as shown in the Hammett plot of Fig. 4*B*. This implies that the rate of steady-state turnover by UGM is indeed sensitive to the electron density at N5 of FAD_{red}. The large negative ρ value suggests a substantial decrease in electron density on the flavin in the transition state of the step(s) that limits steady-state turnover. For the conversion of **2** to **1**, formation of adduct **8** via an S_N2-type reaction (**2** → **8**) and/or formation of the iminium species (**8** → **7**) would involve substantial loss of electron density from the flavin N5 center. If formation of **8** (Fig. 1) were to occur via an S_N1 process, the expectation would be a ρ value approximating zero. Similarly, rate-determining product dissociation in either mechanism would also be expected to yield a ρ value near zero.

Alone, the results of our LFER studies cannot distinguish between rate-limiting S_N2-type adduct formation (**2** → **8**) and iminium formation (**8** → **7**). However, our PIX studies strongly suggest that if an S_N1-type mechanism were operative, then cleavage of the anomeric bond to form an oxocarbenium intermediate (**4**) would be energetically demanding and contribute significantly to limiting k_{cat}. Because this step is significantly impaired when N5 of FAD_{red} is absent in the active site of UGM, the most consistent interpretation of our PIX and LFER studies is that adduct formation (**2** → **8**) occurs by an S_N2-type reaction that is mediated by N5 of FAD_{red}.

In summary, 5-deaza-FAD is not able to support PIX of the β-phosphate oxygens of UDP-Gal*p*, and k_{cat} for the isomerization of UDP-Gal*f* to UDP-Gal*p* exhibits a negative LFER with respect to decreasing electron density at N5 of FAD_{red}. These observations represent a direct experimental evaluation of nucleophilic participation by FAD_{red} during UGM catalysis. Together, they support a mechanism in which the covalent FAD_{red}-Gal*p*/*f* intermediates (**6**/**8**) are formed through a concerted S_N2-type displacement involving N5 of FAD_{red} as the nucleophile. Thus, as has been characterized recently in several other flavoenzymes (14, 26–28), UGM appears to utilize reduced flavin in a covalent manner to mediate chemical transformations that do not involve redox chemistry, illustrating the catalytic versatility of the ubiquitous flavin coenzyme (29). Finally, these findings help explain the pharmacologically unsatisfactory results obtained with UGM inhibitors that mimic a transition state for generation of an oxocarbenium intermediate (5, 30–32). Therefore, analogues that specifically target the nucleophilic addition may offer more promising leads for developing inhibitors of UGM activity.

Acknowledgments—We thank Dr. Kenji Itoh for preparing UDP-Galf and Drs. Ben Shoulders, Yasushi Ogasawara, and Eita Sasaki for helpful suggestions and discussions. We also gratefully acknowledge Steve Sorey for assistance in collecting PIX data.

REFERENCES

1. Richards, M. R., and Lowary, T. L. (2009) Chemistry and biology of galactofuranose-containing polysaccharides. *ChemBioChem.* **10,** 1920–1938
2. Peltier, P., Euzen, R., Daniellou, R., Nugier-Chauvin, C., and Ferrières, V. (2008) Recent knowledge and innovations related to hexofuranosides: structure, synthesis, and applications. *Carbohydr. Res.* **343,** 1897–1923
3. Pan, F., Jackson, M., Ma, Y., and McNeil, M. (2001) Cell wall core galactofuran synthesis is essential for growth of mycobacteria. *J. Bacteriol.* **183,** 3991–3998
4. Gandhi, N. R., Nunn, P., Dheda, K., Schaaf, H. S., Zignol, M., van Soolingen, D., Jensen, P., and Bayona, J. (2010) Multidrug-resistant and extensively drug-resistant tuberculosis: a threat to global control of tuberculosis. *Lancet* **375,** 1830–1843
5. Liautard, V., Desvergnes, V., Itoh, K., Liu, H. W., and Martin, O. R. (2008) Convergent and stereoselective synthesis of imino sugar-containing Gal*f* and UDP-Gal*f* mimics: evaluation as inhibitors of UDP-Gal mutase. *J. Org. Chem.* **73,** 3103–3115
6. Peltier, P., Beláňová, M., Dianišková, P., Zhou, R., Zheng, R. B., Pearcey, J. A., Joe, M., Brennan, P. J., Nugier-Chauvin, C., Ferrières, V., Lowary, T. L., Daniellou, R., and Mikušová, K. (2010) Synthetic UDP-furanoses as potent inhibitors of mycobacterial galactan biogenesis. *Chem. Biol.* **17,** 1356–1366
7. Zhang, Q., and Liu, H. W. (2000) Galactopyranose mutase from *Escherichia coli*: an unusual role of reduced FAD in its Catalysis. *J. Am. Chem. Soc.* **122,** 9065–9070
8. Barlow, J. N., Girvin, M. E., and Blanchard, J. S. (1999) Positional isotope exchange catalyzed by UDP-galactopyranose mutase. *J. Am. Chem. Soc.* **121,** 6968–6969
9. Soltero-Higgin, M., Carlson, E. E., Gruber, T. D., and Kiessling, L. L. (2004) A unique catalytic mechanism for UDP-galactopyranose mutase. *Nat. Struct. Mol. Biol.* **11,** 539–543
10. Gruber, T. D., Westler, W. M., Kiessling, L. L., and Forest, K. T. (2009) X-ray crystallography reveals a reduced substrate complex of UDP-galactopyranose mutase poised for covalent catalysis by flavin. *Biochemistry* **48,** 9171–9173
11. Yuan, Y., Bleile, D. W., Wen, X., Sanders, D. A., Itoh, K., Liu, H. W., and Pinto, B. M. (2008) Investigation of binding of UDP-Gal*f* and UDP-[3-F]Gal*f* to UDP-galactopyranose mutase by STD-NMR spectroscopy, molecular dynamics, and CORCEMA-ST calculations. *J. Am. Chem. Soc.* **130,** 3157–3168
12. Zhang, Q., and Liu, H. (2001) Mechanistic investigation of UDP-galactopyranose mutase from *Escherichia coli* using 2- and 3-fluorinated UDP-galactofuranose as probes. *J. Am. Chem. Soc.* **123,** 6756–6766
13. Itoh, K., Huang, Z., and Liu, H. W. (2007) Synthesis and analysis of substrate analogues for UDP-galactopyranose mutase: implication for an oxocarbenium ion intermediate in the catalytic mechanism. *Org. Lett.* **9,** 879–882
14. Thibodeaux, C. J., Chang, W. C., and Liu, H. W. (2010) Linear free energy relationships demonstrate a catalytic role for the flavin mononucleotide coenzyme of the type II isopentenyl diphosphate:dimethylallyl diphosphate isomerase. *J. Am. Chem. Soc.* **132,** 9994–9996
15. Huang, Z., Zhang, Q., and Liu, H. W. (2003) Reconstitution of UDP-galactopyranose mutase with 1-deaza-FAD and 5-deaza-FAD: analysis and mechanistic implications. *Bioorg. Chem.* **31,** 494–502
16. Midelfort, C. F., and Rose, I. A. (1976) A stereochemical method for detection of ATP terminal phosphate transfer in enzymatic reactions. Glutamine synthetase. *J. Biol. Chem.* **251,** 5881–5887
17. Mullins, L. S., and Raushel, F. M. (1995) Positional isotope exchange as probe of enzyme action. *Method Enzymol.* **249,** 398–425
18. Taft, R. W., Jr., Ehrenson, S., Lewis, I. C., and Glick, R. E. (1959) Evaluation of resonance effects on reactivity by application of the linear inductive energy relationship. VI. Concerning the effects of polarization and conjugation on the mesomeric Order. *J. Am. Chem. Soc.* **81,** 5352–5361
19. Edmondson, D. E., and Ghisla, S. (1999) *Flavins and Flavoproteins*, pp. 71–76, Agency for Scientific Publications, Berlin
20. Walsh, C. (1986) Naturally occurring 5-deazaflavin coenzymes: biological redox roles. *Acc. Chem. Res.* **19,** 216–221
21. Hansch, C., Leo, A., and Taft, R. W. (1991) A survey of Hammett substituent constants and resonance and field parameters. *Chem. Rev.* **91,** 165–195
22. Taft, R. W., Jr. (1960) Sigma values from reactivities. *J. Phys. Chem.* **64,** 1805–1815
23. Yorita, K., Misaki, H., Palfey, B. A., and Massey, V. (2000) On the interpretation of quantitative structure-function activity relationship data for lactate oxidase. *Proc. Natl. Acad. Sci. U.S.A.* **97,** 2480–2485
24. Roth, J. P., Wincek, R., Nodet, G., Edmondson, D. E., McIntire, W. S., and Klinman, J. P. (2004) Oxygen isotope effects on electron transfer to O_2 probed using chemically modified flavins bound to glucose oxidase. *J. Am. Chem. Soc.* **126,** 15120–15131
25. Legrand, Y. M., Gray, M., Cooke, G., and Rotello, V. M. (2003) Model systems for flavoenzyme activity: relationships between cofactor structure, binding, and redox properties. *J. Am. Chem. Soc.* **125,** 15789–15795
26. Yu, Q., Schaub, P., Ghisla, S., Al-Babili, S., Krieger-Liszkay, A., and Beyer, P. (2010) The lycopene cyclase CrtY from *Pantoea ananatis* (formerly *Erwinia uredovora*) catalyzes an FAD_{red}-dependent non-redox reaction. *J. Biol. Chem.* **285,** 12109–12120
27. Kommoju, P. R., Bruckner, R. C., Ferreira, P., and Jorns, M. S. (2009) Probing the role of active site residues in NikD, an unusual amino acid oxidase that catalyzes an aromatization reaction important in nikkomycin

biosynthesis. *Biochemistry* **48,** 6951–6962
28. Rauch, G., Ehammer, H., Bornemann, S., and Macheroux, P. (2007) Mutagenic analysis of an invariant aspartate residue in chorismate synthase supports its role as an active site base. *Biochemistry* **46,** 3768–3774
29. Mansoorabadi, S. O., Thibodeaux, C. J., and Liu, H. W. (2007) The diverse roles of flavin coenzymes: nature's most versatile thespians. *J. Org. Chem.* **72,** 6329–6342
30. Caravano, A., Vincent, S. P., and Sinaÿ, P. (2004) Efficient synthesis of a nucleoside-diphospho-exo-glycal displaying time-dependent inactivation of UDP-galactopyranose mutase. *Chem. Commun.* 1216–1217
31. Caravano, A., Dohi, H., Sinaÿ, P., and Vincent, S. P. (2006) A new methodology for the synthesis of fluorinated *exo*-glycals and their time-dependent inhibition of UDP-galactopyranose mutase. *Chem. Eur. J.* **12,** 3114–3123
32. Desvergnes, S., Desvergnes, V., Martin, O. R., Itoh, K., Liu, H. W., and Py, S. (2007) Stereoselective synthesis of β-1-C-substituted 1,4-dideoxy-1,4-imino-D-galactitols and evaluation as UDP-galactopyranose mutase inhibitors. *Bioorg. Med. Chem.* **15,** 6443–6449